J Appl Electrochem (2014) 44:491–496
DOI 10.1007/s10800-013-0647-x

RESEARCH ARTICLE

Leakage currents and self-discharge of ionic liquid-based supercapacitors

Francesca Soavi · Catia Arbizzani · Marina Mastragostino

Received: 24 July 2013 / Accepted: 20 November 2013 / Published online: 27 November 2013

Abstract Ionic liquid (IL)-based supercapacitors have been widely demonstrated to outperform electrochemical double-layer capacitors (EDLCs) working with conventional organic electrolytes in terms of specific energy and operating voltage. Here, the results of a study on the leakage currents (I_{leak}) and self-discharge energy loss factors (SDLF) of IL-based EDLCs at different cell voltages up to 3.2 V and at 30° and 60 °C are reported. Cells assembled with the *N*-butyl-*N*-methyl-pyrrolidinium bis(trifluoromethanesulfonyl) imide ($PYR_{14}TFSI$) and *N*-methoxyethyl-*N*-methylpyrrolidinium bis(trifluoromethanesulfonyl)imide pure ILs and a mixture of $PYR_{14}TFSI$ and propylene carbonate (PC) 1 to 1 molar were tested. The results are compared to those achieved with EDLCs featuring the conventional 1 M tetraethyl ammonium tetrafluoroborate (Et_4NBF_4)-PC electrolyte. The study demonstrates that ILs provide I_{leak} and SDLF that are lower than those obtained with the latter electrolyte, with $PYR_{14}TFSI$ allowing the lowest values.

Keywords Supercapacitor · Ionic liquid · Self-discharge · Leakage current · EDLC

1 Introduction

Supercapacitors are under consideration for applications ranging from transportation to stand-alone or grid-connected power plants as well as for hand-held electronic devices and miniaturized autonomous electronic equipments. Different size of these systems implies capacitance, delivered energy and power, and discharge times and rate that can differ by more than three orders of magnitude. Supercapacitors are investigated focusing the studies on their discharge behavior and little attention is paid to self-discharge. But different applications also means different charge mode, charge current, and rest time that should be set according to leakage currents and self-discharge at rated voltage. High recharge efficiency requires that constant current (CC)–constant voltage (CV) charge mode has CV leakage currents that are 10 % lower than the CC charge currents. This is critical for effective recharges of miniaturized systems that involve very low charge currents [1]. Self-discharge of a charged supercapacitor in rest mode is important for applications where the supercapacitors are not connected to an electrical network which could maintain their state of charge. The self-discharge may be due to leakage currents and charge redistribution, which in turn reflects on cell voltage variation over time and is affected by rated voltage and temperature [2, 3]. The different self-discharge of series-connected cells affects voltage distribution in the module under operation and rest, and this is particularly critical for reliability, safe operation, and cycle and calendar life of large size modules like those for hybrid electric vehicles [4].

The use of IL-based electrolytes has been demonstrated to improve the supercapacitor energy delivered at high voltages and power rates both of large size and micro-systems with the added advantage of a high safety due to their thermal and chemical stability [5, 6]. Here, the results of a study on the self-discharge and leakage currents of IL-based double-layer carbon supercapacitors (EDLCs) are reported. The study is focused on the *N*-butyl-*N*-methyl-pyrrolidinium bis(trifluoromethanesulfonyl) imide ($PYR_{14}TFSI$) and *N*-methoxyethyl-*N*-methylpyrrolidinium bis(trifluoromethanesulfonyl)imide ($PYR_{1(2O1)}TFSI$) pure ILs, on a mixture of $PYR_{14}TFSI$ and propylene carbonate (PC) 1 to 1 molar, and the results are

F. Soavi (✉) · C. Arbizzani · M. Mastragostino
Dipartimento di Chimica "Giacomo Ciamician", via Selmi 2, 40126 Bologna, Italy
e-mail: francesca.soavi@unibo.it

compared to those achieved with the conventional 1 M tetraethyl ammonium tetrafluoroborate (Et_4NBF_4)-PC electrolyte.

2 Experimental

The $PYR_{14}TFSI$ (99.5 %, Solvionic) and $PYR_{1(2O1)}TFSI$ (Evonik Industries) ILs and the 1 M Et_4NBF_4-PC solution (Mitsubishi Chemical Co) were used as received; the PC:$PYR_{14}TFSI$ 1:1 mol solution was prepared with PC that was distilled under vacuum.

The EDLCs were assembled as in Ref. [7] with composite electrodes (0.64 cm^2) with 90 % w/w carbon-10 % w/w polytetrafluoroethylene and carbon-coated aluminum current collectors. The electrodes were cut from laminated belts produced by Leclanché Lithium under the ILHYPOS EU project.

The activated carbon (AC) was PICACTIF SUPERCAP BP10 (Pica) treated at 1,050 °C in Ar for 2 h; the carbon displayed a total pore volume of 1.2 $cm^3\ g^{-1}$ with a pore size distribution centered at 2.7 nm. The positive to negative electrode composite loading ratio was 1.6, and the total composite mass of the two electrodes (m_{EDLC}) was 16.8 mg cm^{-2}; a different mass loading of the positive and the negative electrode was used in order to achieve cell voltages higher than 3 V. The EDLCs featured a T Swagelok-type cell assembly with an Ag quasi-reference electrode disk and were assembled in a dry box (MBraun Labmaster 130, H_2O, and $O_2 < 1$ ppm) using a fiber glass filter as a separator (Whatman GF/F); the separator and electrodes were soaked under vacuum with the IL before the assembly.

The electrochemical tests were performed at room temperature (RT) or in thermostatic oven at 30° and 60 °C using a BioLogic VSP multichannel potentiostat/galvanostat/FRA. Electrochemical impedance spectroscopy was performed with 50–10 mHz frequency range and 5 mV ac perturbation, acquiring 10 points per decade.

Thermogravimetric analyses (TGA) were performed with a TA Instruments Q50 System in the temperature range of 25–600 °C at a scanning rate of 20 °C min^{-1} in N_2.

3 Results and discussion

The electrochemical stability windows (ESWs) at glassy carbon electrode (GC) of $PYR_{14}TFSI$, $PYR_{1(2O1)}TFSI$, PC:$PYR_{14}TFSI$ 1:1, and PC-1 M Et_4NBF_4 electrolytes are wider than 5 V and the ionic conductivities at RT increase in the order $PYR_{14}TFSI$ (2.5 mS cm^{-1}) <$PYR_{1(2O1)}TFSI$ (3.8 mS cm^{-1}) <PC:$PYR_{14}TFSI$ 1:1 ≅ PC- 1 M Et_4NBF_4 (12 and 14 mS cm^{-1}, respectively) [7–10]. Figure 1 reports

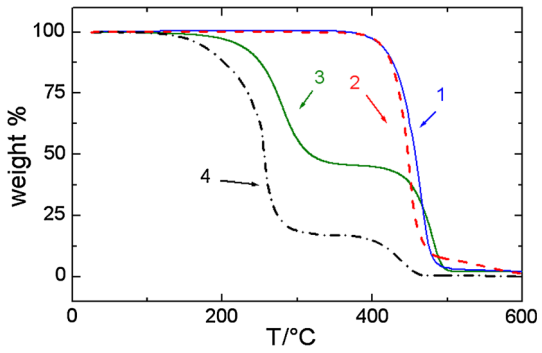

Fig. 1 TGA plots of the $PYR_{14}TFSI$ (*1*), $PYR_{1(2O1)}TFSI$ (*2*), PC:$PYR_{14}TFSI$ 1:1 (*3*), PC: 1 M EtN_4BF_4 (*4*) electrolytes

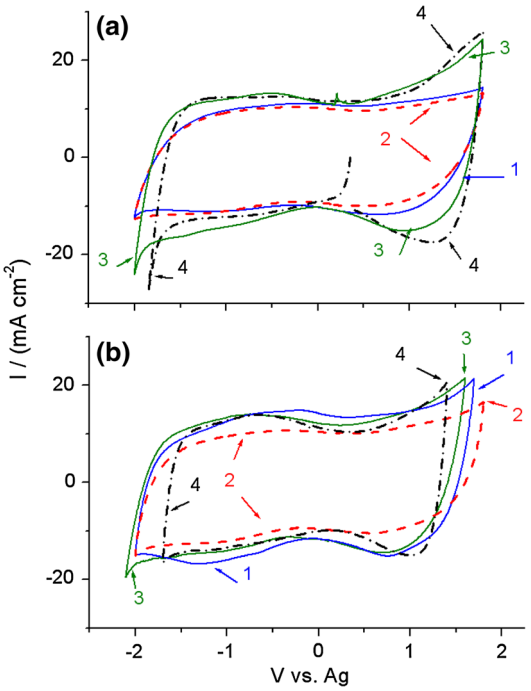

Fig. 2 Cyclic voltammograms in 3-electrode mode of AC electrodes (6.3 mg cm^{-2}) in $PYR_{14}TFSI$ (*1*), $PYR_{1(2O1)}TFSI$ (*2*), PC:$PYR_{14}TFSI$ 1:1 (*3*), PC: 1 M EtN_4BF_4 (*4*) at 20 mV s^{-1} and **a** RT and **b** 60 °C

the TGA plots of the investigate electrolytes and evidences that the pure ILs are much more stable than the solutions with PC; the TGA mass loss of the PC:$PYR_{14}TFSI$ 1:1 mixture is at higher temperatures than that of PC- 1 M Et_4NBF_4 mainly because of the higher ion concentration, and hence, lower vapor pressure of the former electrolyte than that of the latter.

The ESW and electrolyte conductivity affect the supercapacitor maximum rated voltage and equivalent series resistance (ESR) that also depend on the nature of the carbon electrodes.

The cyclic voltammograms in 3-electrode mode reported in Fig. 2 indicate that the AC electrode can be charged/

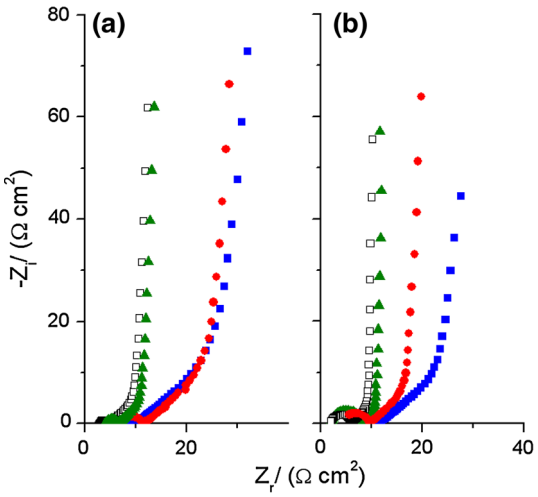

Fig. 3 Nyquist plots of the EDLCs assembled with $PYR_{14}TFSI$ (*solid square*), $PYR_{1(2O1)}TFSI$ (*circle*), PC:$PYR_{14}TFSI$ 1:1 (*triangle*), PC: 1 M EtN_4BF_4 (*open square*) at **a** RT and **b** 60 °C (50–10 mHz frequency range)

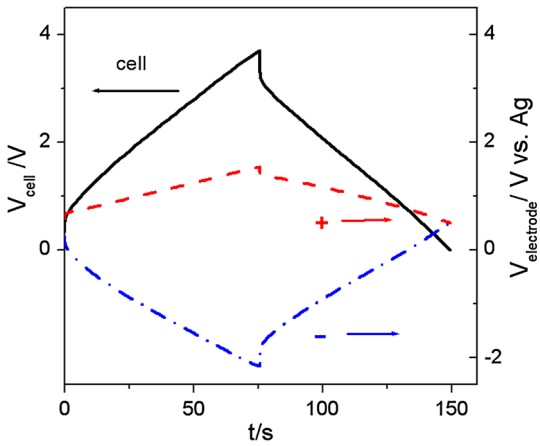

Fig. 4 Cell voltage (*solid line*, *left* axis) and positive (*dashed line*, *right* axis) and negative (*dot-dashed line*, *right* axis) electrode potential profiles of the EDLC with PC:$PYR_{14}TFSI$ 1:1 under galvanostatic cycling at ca 1 A g^{-1} and RT

discharged with a coulombic efficiency higher than 95 % at current densities of ca. 10 mA cm^{-2} within a potential excursion narrower than 4 V, i.e., much narrower than the ESW at GC, in agreement with the literature on the evaluation of the electrochemical stability of the electrolytes at high surface area carbon electrodes [11]. At 60 °C, the voltammetric currents increase in the case of the pure ILs and the electrode potential excursion for having a high charge/discharge efficiency narrows by ca. 100–200 mV.

Figure 3 shows the Nyquist plots of the EDLCs assembled with the different electrolytes. The plots evidence that the ESR is mainly affected by the Warburg impedance which is due to ion diffusion in the porous electrodes. Such impedance contribution is higher for the cells with the pure ILs with respect to those with PC. At RT, the ESR evaluated at the frequency where the limit capacitance is reached (ca. 50 mHz) is ca 25 Ω cm^2 for the systems with the pure ILs and 10 Ω cm^2 for those with PC and in the case of the former electrolytes it slightly decreases by temperature rise at 60 °C.

As an example, Fig. 4 shows the cell voltage and electrode potential profiles of the EDLC with PC:$PYR_{14}TFSI$ 1:1 under galvanostatic cycling at ca. 1 A g^{-1} and RT up to 3.7 V. The different electrode loadings of the positive and negative electrodes allow to reach cell voltages (V_0) higher than 3 V with all the electrolytes and up to 3.8 V with $PYR_{14}TFSI$; with PC- 1 M Et_4NBF_4, the highest V_0 for a coulombic efficiency >98 % was 3.2 V. The specific capacitance (C) and maximum specific energy ($E_{max} = {}^1/_2CV_0^2$) of the IL-based EDLCs were similar and of ca. 20 F g^{-1} and 40 Wh kg^{-1} at $V_0 = 3.7$ V, respectively. At 3.2 V, the E_{max} of the cell with PC- 1 M Et_4NBF_4 was 30 Wh kg^{-1}. The maximum specific power ($P_{max} = V_0/(4ESRm_{EDLC})$) ranged from 8 kW kg^{-1} for the EDLCs with the pure ILs up to 15 and 20 kW kg^{-1} for those with PC- 1 M Et_4NBF_4 and PC:$PYR_{14}TFSI$ 1:1, respectively, which are the cells featuring the lowest ESRs.

According to the FreedomCAR Ultracapacitor Test Manual [12], the CC–CV test at low currents is a reference for the evaluation of the maximum supercapacitor discharge performance (RCT, reference capacity test). The test consists of a charge at ca. 5C constant current (I_{RCT}, 0.9 mA cm^{-2} corresponding to ca. 50 mA g^{-1}, CC step) up to a voltage that is clamped for 1 h or until the current reaches 10 % of I_{RCT} (CV step). Then, the EDLC is discharged at the same I_{RCT} current than charge. The CC–CV charge protocol is designed to approach the theoretical maximum energy storage capability of the systems by minimizing iR ohmic overpotentials. But this has also the detrimental effect of kinetically favoring side, irreversible electrochemical decomposition of the electrolyte at much lower cell voltage than the maximum voltage which is feasible by continuous, fast galvanostatic cycling (see Fig. 4) [13]. Indeed, Fig. 5 reports the cell voltage and current profiles of the 4 supercapacitors under the RCT tests and shows that at such low currents the charge cannot be performed above 3.5 V because of the onset of faradic processes evidenced by cell voltage bending during the CC charge step. Such processes even caused not negligible CV leakage currents and CC–CV recharge efficiency dramatically low. Table 1 reports V_0, the discharge capacitance (C_{RCT}) and energy ($E_{RCT} = I_{RCT}\int V(t)\,dt$) densities, and the coulombic efficiency (η) evaluated by the RCT discharge curves reported in Fig. 5. While the very low values of η are affected by the use of not optimized laboratory cells which feature excess electrolyte, Table 1 indicates that the electrolytes which permit the highest V_0 are the pure ILs.

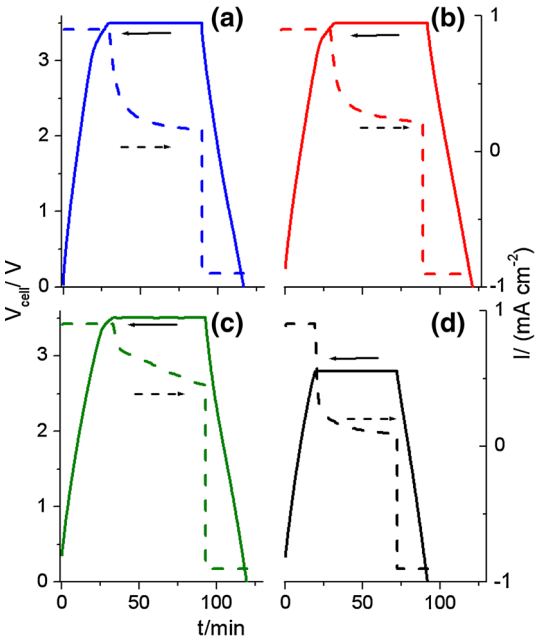

Fig. 5 Cell voltage (*solid lines*) and current (*dashed lines*) profiles of the EDLCs assembled with $PYR_{14}TFSI$ (**a**), $PYR_{1(2O1)}TFSI$ (**b**), PC:$PYR_{14}TFSI$ 1:1 (**c**), PC: 1 M EtN_4BF_4 (**d**) under the CC–CV, RCT tests at 30 °C

Table 1 Voltage (V_0), discharge capacitance (C_{RCT}) and energy (E_{RCT}) densities, and coulombic efficiency from RCT tests at 30 °C

Electrolyte	V_0 V	C_{RCT} F cm^{-2}	E_{RCT} mWh cm^{-2}	η %
$PYR_{14}TFSI$	3.5	0.44	0.63	58
$PYR_{1(2O1)}TFSI$	3.5	0.47	0.72	56
PC:$PYR_{14}TFSI$ 1:1	3.5	0.45	0.65	37
PC- 1 M Et_4NBF_4	2.8	0.39	0.42	69

The leakage currents (I_{leak}) and self-discharge of the supercapacitors were investigated at different V_0 by the protocol described in Ref. [12]. It consists of a slow galvanostatic charge at 5C up to a V_0 that is held over 72 h, followed by rest over 72 h, and by discharge at the same current as charge. Figure 6a shows the values of the leakage currents rated to the RCT capacitance ($I_{leak}' = I_{leak}/C_{RCT}$) over the CV time at 2.8 V and 30 °C. After 72 h, the lowest I_{leak}' is reached by the two systems featuring $PYR_{14}TFSI$, pure and mixed with PC. Despite the low cell voltage (1 V lower than that feasible by galvanostatic cycling), the minimum currents are much higher than the target value of 1 μA per Farad, which is suggested for commercial systems [2]. However, these results might be ameliorated by a better laboratory cell assembly. Table 2 reports the I_{leak}' values after 72 h at different V_0, which provide indications about the feasible lowest current for an

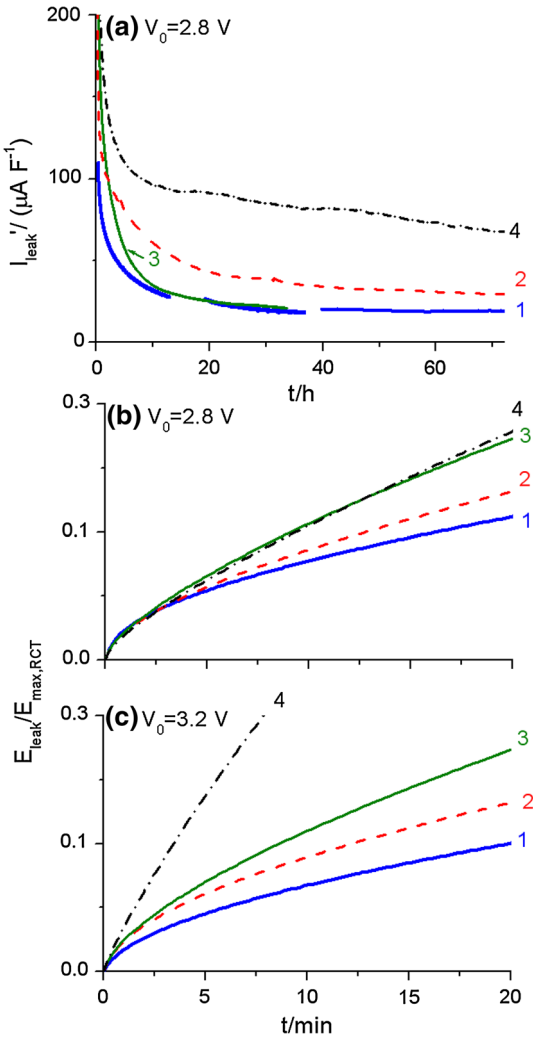

Fig. 6 Trends over the CV time at 30 °C of the leakage current rated to the EDLC capacitance ($I_{leak}' = I_{leak}/C_{RCT}$) at 2.8 V (**a**) and of the leakage energy normalized to the maximum deliverable energy ($E_{leak}/E_{max,\ RCT}$) at **b** 2.8 V and **c** 3.2 V of the EDLCs assembled with $PYR_{14}TFSI$ (*1*), $PYR_{1(2O1)}TFSI$ (*2*), PC:$PYR_{14}TFSI$ 1:1 (*3*), and PC: 1 M EtN_4BF_4 (*4*)

effective recharge of the supercapacitor. An effective recharge requires that the charge stored during the CC step is at least 10 times higher than the charge that can be simultaneously dissipated for leakage. Hence, the minimum charge current should be 10 times higher than I_{leak}, i.e., higher than 8 mA g^{-1} for the EDLC with $PYR_{14}TFSI$ which features an I_{leak} of 0.75 mA g^{-1} at 3.2 V and a C_{RCT} of 0.44 F cm^{-2}.

The leakage currents are used to calculate the leakage resistances (R_p) that are in parallel with the double-layer charging process by $R_p = V_0/I_{leak}$ and the data are also reported in Table 2. For all the systems R_p increases with V_0; the EDLCs featuring the highest values are those based on $PYR_{14}TFSI$.

Table 2 Leakage current rated to the EDLC capacitance ($I_{leak}' = I_{leak}/C_{RCT}$) and leakage resistance (R_p) after 72 h, CV time for $E_{leak}/E_{max,RCT}$ <0.1 and rest time for self-discharge energy loss factor (SDLF) <0.1 at the rated V_0 voltages and 30 °C

Electrolyte	V_0 V	I_{leak} '@ 72 h μA F^{-1}	R_p @ 72 h kΩ cm^2	CV time for $E_{leak}/E_{max,RCT} < 0.1$ min	Rest time for SDLF <0.1 min
$PYR_{14}TFSI$	2.8	20	355	8	87
	3.2	30	245	10	68
$PYR_{1(2O1)}TFSI$	2.8	30	200	7	73
	3.2	85	80	6	27
PC:$PYR_{14}TFSI$ 1:1	2.8	20[a]	295	5	118
	3.2	35	195	5	64
PC-1 M Et_4NBF_4	2.8	65	107	5	36
	3.2	90	90	2	23

[a] after 33 h

Integration of I_{leak} over time gives the leakage charge that, multiplied by V_0, provides the leakage energy ($E_{leak}(t) = V_0 \int I_{leak}(t)\,dt$), i.e., the energy dissipated to keep the supercapacitor at a given state of charge. Figure 6b, c show the trends over time of E_{leak} normalized to the maximum deliverable energy $E_{max,\,RCT}$ ($E_{max,\,RCT} = \frac{1}{2}C_{RCT}V_0^2$) for the different systems at different V_0 and 30 °C. The plots are cut at 20 min to better highlight which is the maximum duration of the CV step that provides E_{leak} lower than 10 % of $E_{max,\,RCT}$. The maximum CV times that allow 90 % charge efficiency at given V_0 are summarized in Table 2. At 3.2 V, it is not very effective to keep the cell charged for more than 10 min. At the beginning of the CC step, the presence of PC worsens the charge efficiency and this in agreement with the narrower ESW at AC of PC-based electrolytes than that of pure ILs. The fact that after 72 h the leakage resistance of the cell with PC:$PYR_{14}TFSI$ 1:1 is higher than that of the EDLC with $PYR_{1(2O1)}TFSI$ can be explained with electrode passivation promoted by PC.

Figure 7a shows the trends of the cell voltages over time during the rest step that follows the CC–CV charge at 30 °C and $V_0 = 2.8$ V. At such voltage, the systems which retain the charge for longer time are those based on $PYR_{14}TFSI$. Elaboration of the cell voltage over time in rest conditions provided the self-discharge energy loss factor (SDLF), i.e., the ratio of the energy lost over time to the maximum energy deliverable at the beginning of rest. SDLF was calculated by $SDLF(t) = 1 - (V(t)/V_0)^2$. Figure 7b, c show the SDLF trends over time cut at 1 h, and Table 2 reports the maximum rest times that should be adopted for a self-discharge lower than 90 % at 30 °C. The systems with $PYR_{14}TFSI$-based electrolyte are the best performing and the EDLC with pure $PYR_{14}TFSI$ is less affected by the increase of cell voltage. With pure $PYR_{14}TFSI$ the cell can be left in rest over 1.5 and 1 h at 2.8 and 3.2 V, respectively.

Leakage current and self-discharge tests were even carried out at 60 °C, and the results for the IL-based

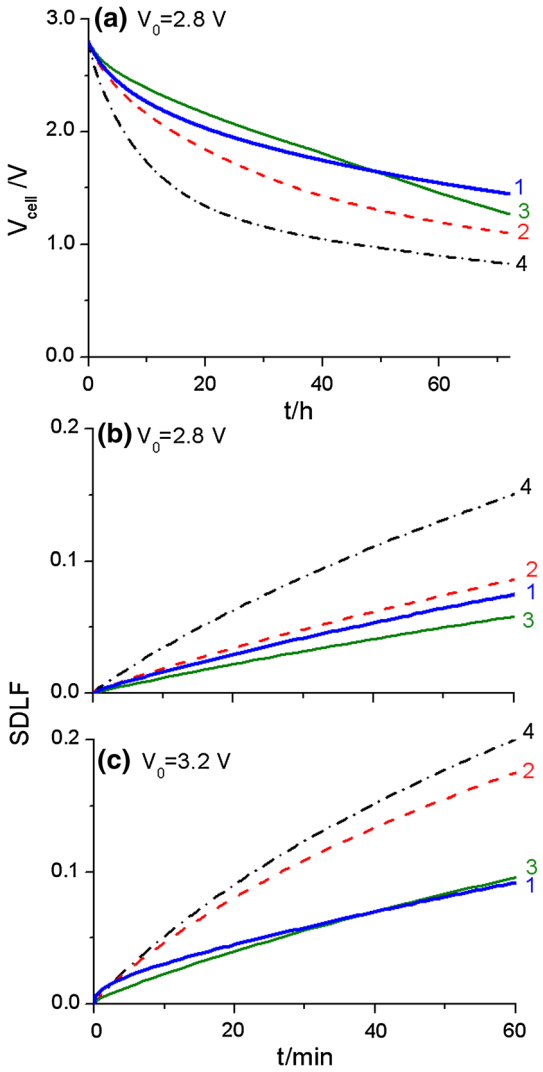

Fig. 7 Trends over the rest time at 30 °C of the cell voltages after charge at 2.8 V(**a**) and of the self-discharge energy loss factors (SDLF) with V_0 of **b** 2.8 V and **c** 3.2 V of the EDLCs assembled with $PYR_{14}TFSI$ (*1*), $PYR_{1(2O1)}TFSI$ (*2*), PC:$PYR_{14}TFSI$ 1:1 (*3*), and PC: 1 M EtN_4BF_4 (*4*)

Table 3 Leakage current rated to the EDLC capacitance ($I_{leak}' = I_{leak}/C_{RCT}$) and leakage resistance (R_p) after 72 h, CV time for $E_{leak}/E_{max,RCT} < 0.1$ and rest time for self-discharge energy loss factor (SDLF) < 0.1 at the rated V_0 voltages and 60 °C of the IL-based EDLCs

Electrolyte	V_0 V	I_{leak}'@ 72 h μA F^{-1}	R_p @ 72 h kΩ cm^2	CV time for $E_{leak}/E_{max,RCT} < 0.1$ min	Rest time for SDLF < 0.1 min
$PYR_{14}TFSI$	2.8	50	130	3	40
	3.2	100	70	3	20
$PYR_{1(2O1)}TFSI$	2.8	110	60	3	25
	3.2	275	25	4	7
PC:$PYR_{14}TFSI$ 1:1	2.8	140	45	2	15
	3.2	450	15	2	3

EDLCs are summarized in Table 3. The I_{leak} and SDLF increase with temperature and V_0 and the trends within the different electrolytes are maintained. $PYR_{14}TFSI$ is still the best performing system, but at 60 °C the CV step and rest times should be shortened down to less than 5 min and 1 h, respectively.

4 Conclusions

Cell voltages of IL-based EDLCs higher than 3.5 V are feasible in "galvanostatic cycling" conditions by the use of positive and negative electrodes of different weight. However, the maximum cell voltage in CC–CV charge mode at low charge rates should be lower than that achievable by continuous galvanostatic cycling and the CV time at such voltage should be set according to I_{leak}. In 0.4 F cm^{-2} lab cells with $PYR_{14}TFSI$, charge efficiency higher than 90 % is achievable if the I_{RCT} current is higher than 8 mA g^{-1} and the CV time at 3.2 V is 10 min at maximum. These cells should be kept in rest at 3.2 V less than 1 h in order to recover the 90 % of the deliverable energy.

The IL-based EDLCs, and particularly the one with pure $PYR_{14}TFSI$, feature I_{leak} and SDLF which are lower and less affected by the temperature than those of the cell with the PC- 1 M Et_4NBF_4 conventional organic electrolyte.

Acknowledgments The authors would thank Dr. K.H Pettinger and Dr. M. Conte for the fruitful collaboration under the ILHYPOS "Ionic Liquid-based Hybrid Supercapacitor" UE Project (Contract No. TST4-CT-2005-518307).

References

1. Mars P (2012) Coupling a supercapacitor with a small energy-harvesting source. EDN, June 7:39–42. http://www.edn.com
2. Kötz R, Hahn M, Gallay R (2006) Temperature behavior and impedance fundamentals of supercapacitors. J Power Sources 154:550–555. doi:10.1016/j.jpowsour.2005.10.048
3. Diab Y, Venet P, Gualous H, Rojat G (2009) Self-discharge characterization and modeling of electrochemical capacitor used for power electronics applications. IEE Trans Power Electron 24:511–517. doi:10.1109/TPEL.2008.2007116
4. Kötz R, Sauter JC, Ruch P, Dietrich P, Büchi FN, Magne PA, Varenne P (2007) Voltage balancing: long-term experience with the 250 V supercapacitor module of the hybrid fuel cell vehicle HY-LIGHT. J Power Sources 174:264–271. doi:10.1016/j.jpowsour.2007.08.078
5. Lazzari M, Arbizzani C, Soavi F, Mastragostino M (2013) EDLCs based on solvent-free ionic liquids. In: Beguin F, Frackowiak E (eds) Supercapacitors: materials, systems and applications. Wiley-VCH Verlag GmbH &Co, KGaA, Weinheim, pp 289–306
6. Kang YJ, Chun SJ, Lee SS, Kim BY, Kim JH, Chung H, Lee SY, Kim W (2012) All-solid-state flexible supercapacitors fabricated with bacterial nanocellulose papers, carbon nanotubes, and tri-block-copolymer ion gels. ACS Nano 6:6400–6406. doi:10.1021/nn301971r
7. Lazzari M, Soavi F, Mastragostino M (2009) Dynamic pulse power and energy of ionic-liquid-based supercapacitor for HEV application. J Electrochem Soc 156:A661–A666. doi:/10.1149/1.3139046
8. Krause A, Balducci A (2011) High voltage electrochemical double layer capacitor containing mixtures of ionic liquids and organic carbonate as electrolytes. Electrochem Commun 13:814–817. doi:/10.1016/j.elecom.2011.05.010
9. Ruiz V, Huynh T, Sivakkumar SR, Pandolfo AG (2012) Ionic liquid-solvent mixtures as supercapacitor electrolytes for extreme temperature operation. RSC Adv 12:5591–5598. doi:10.1039/c2ra20177a
10. Ue M, Takeda M, Takehara M, Mori S (1997) Electrochemical properties of quaternary ammonium salts for electrochemical capacitors. J Electrochem Soc 144:2684–2688. doi:10.1149/1.1837882
11. Weingarth D, Noh H, Foelske-Schmitz A, Wokaun A, Kötz R (2013) A reliable determination method of stability limits for electrochemical double layer capacitors. Electrochim Acta 103:119–124. doi:10.1016/j.electacta.2013.04.057
12. INEEL (2004) FreedomCAR Ultracapacitor Test Manual, Prepared for the US Department of Energy. http://www.uscar.org/commands/files_download.php?files_id=28. Accessed 25 Nov 2013
13. Weingarth D, Foelske-Schmitz A, Kötz R (2013) Cycle versus voltage hold: which is the better stability test for electrochemical double layer capacitors? J Power Sources 225:84–88. doi:10.1016/j.powsour.2012.10.019